

Facile method for synthesis of mixed-cation halide perovskites by mild equilibrium conversion *via* iodine-mediated transport reaction in inert liquid media

Sergey A. Fateev,^{a,†} Anna D. Riabova,^{a,†} Eugene A. Goodilin^{a,b} and Alexey B. Tarasov^{*a,b}

^a Department of Materials Science, M. V. Lomonosov Moscow State University, 119991 Moscow, Russian Federation. E-mail: alexey.bor.tarasov@yandex.ru

^b Department of Chemistry, M. V. Lomonosov Moscow State University, 119991 Moscow, Russian Federation

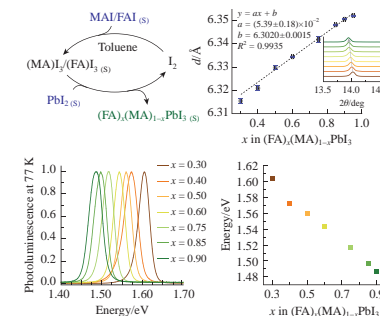
DOI: 10.1016/j.mencom.2023.04.004

A new facile method for the synthesis of mixed-cation halide perovskites based on the chemical conversion of solid precursors (organic halides and lead halides) *via* an iodine-mediated transport reaction in inert liquid media under mild conditions is described. The equilibrium nature of the conversion provides an exact match between the stoichiometry of the resulting perovskite powder and the molar ratio of the precursors. This method can serve as a useful tool for the synthesis of complex perovskite precursors and the investigation of phase equilibria.

Keywords: hybrid halide perovskites, polyiodides, solid solutions, solid phase equilibria, perovskite photovoltaics.

In the last decade, semiconductor materials based on lead halide perovskites APbX_3 (A is a singly charged cation, X is a halide anion) have aroused great interest in the scientific community due to the unique set of optoelectronic properties^{1–4} and relatively simple synthetic procedures,⁵ which provides high prospects for practical applications of this class of materials. Perovskite solar cells (PSCs) are considered as a new generation of photovoltaic devices, characterized by high chances of transition to practical use in the foreseeable future due to the achievement of high efficiency up to 25.7% for single-junction PSCs and 32.5% for ‘perovskite–silicon’ tandem solar cells.⁶ Along with the optimization of architectures and functional layers of PSCs, such high efficiencies were achieved through careful optimization of the cationic and anionic composition of APbX_3 perovskite, during which solid solutions based on formamidinium (FA^+) cations with methylammonium (MA^+) and Cs^+ additives were selected as the best compositions, in some cases also with partial replacement of iodine by bromine.⁷

Despite a fairly large number of works devoted to the study of the compositional space of lead halide perovskites, most of our knowledge about the phase assemblage and properties of such compositions is based on the study of thin films obtained under extremely non-equilibrium conditions (fast crystallization, sharp annealing). The use of single crystals also does not help to establish the true thermodynamic equilibrium state of complex compositions, since the growth of crystals is also carried out mainly from organic solvents,⁸ which not only form strong complexes and solvates with perovskite components,⁹ but are also capable of significantly changing the phase transition temperatures, intercalating into the structure and stabilizing metastable phases.¹⁰ Moreover, due to the high reactivity of FA^+ cations, even precipitation from aqueous



solutions of hydrohalic acids is accompanied by chemical reactions of FA^+ cations with each other and the formation of by-products.¹¹

In addition to all of the above, the application of the classical approach to achieve thermodynamic phase equilibrium for solid phases, *i.e.*, high-temperature sintering, in the case of hybrid halide perovskites is also difficult due to their poor thermal stability.¹² Thus, although the study of phase relationships and stability limits of solid solutions such as $(\text{FA})_x(\text{MA})_{1-x}\text{PbI}_{3-y}\text{Br}_y$ under equilibrium conditions is an urgent task, the existing methods of synthesis are far from the conditions of thermodynamic equilibrium. In this work, we have proposed a method for obtaining perovskite powders of the exact cationic composition $(\text{FA})_x(\text{MA})_{1-x}\text{PbI}_3$ under mild and equilibrium conditions, excluding the degradation of cations and the participation of a solvent, and characterized the structural and optical properties of the resulting solid solutions.

The concept of the proposed method is to use a mediator or mass transfer agent to achieve chemical equilibrium between solid precursors (MAI, FAI, PbI₂) dispersed in an inert liquid medium. Toluene was chosen as the latter, which is nonpolar, noncoordinating and does not form hydrogen bonds.¹³ We initially selected three different mediators, *N,N*-dimethylformamide (DMF), isopropanol (IPA) and iodine (I₂), to test their effect on the formation of a typical hybrid perovskite, MAPbI_3 .[‡] All three compounds are able to partially transfer the components of the system into a liquid phase and provide mass transfer: DMF due to the formation of complexes with iodoplumbate ions, IPA due to the solvation of organic cations¹³ and iodine due to the formation of soluble polyiodides.¹⁴ All three mediators were added to toluene in an amount of 5 mol% of the amount of lead, and IPA and DMF were

[‡] MAI (Dyesol), FAI (Dyesol) and PbI₂ (99.999%, Lanhit) were purchased commercially and used without further purification. The solvents DMF, IPA and toluene were dried over molecular sieves before use.

[†] These authors contributed equally to this work.

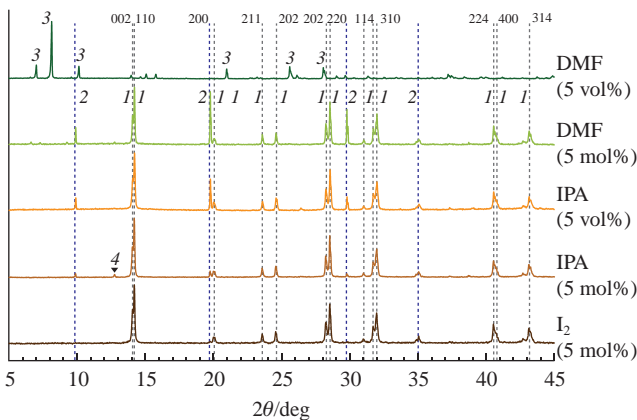


Figure 1 X-ray diffraction patterns of MAPbI_3 powders obtained with different mediators (shown on the right) in an amount of 5 vol% of toluene or 5 mol% of the amount of lead. Reflection peak positions: (1) MAPbI_3 (main), (2) MAI ($h00$), (3) $(\text{MA})_2\text{Pb}_3\text{I}_8 \cdot 2\text{DMF}$ and (4) PbI_2 .

also added in an amount of 5 vol% of toluene. The ratio of PbI_2 to toluene for all syntheses was 0.3 mmol per 1 ml. For synthesis, the precursors, toluene and mediator were placed in the specified ratio in a sealed glass vial and left under vigorous stirring and heating up to 70 °C for 5 days. After that, the mixture was extracted; the perovskite powder was separated from the liquid, washed twice with fresh toluene and dried in a dry box.

As can be seen from the XRD⁸ data (Figure 1), when DMF is used as a mediator, the adduct phase $(\text{MA})_2\text{Pb}_3\text{I}_8 \cdot 2\text{DMF}$ ¹⁵ is inevitably formed. In the case of IPA, the simultaneous formation of MAI and PbI_2 impurities is observed, presumably due to partial extraction of MAI with IPA and subsequent separate crystallization. And only iodine makes it possible to obtain single-phase perovskite MAPbI_3 as a synthesis product. Additionally, as we have shown earlier, I_2 at moderate concentrations does not impair, but even improves the internal properties of hybrid lead iodide perovskites.^{16,17} Therefore, the toluene–iodine system was subsequently used for the synthesis of mixed cationic perovskites $(\text{FA})_x(\text{MA})_{1-x}\text{PbI}_3$. It is based on the following chemical equilibria:



Notably, the melts known for MA and FA polyiodides¹⁸ do not form *per se* because of the low iodine concentration (0.015 M) and the very low solubility of polyiodides in toluene.¹⁹ Based on the

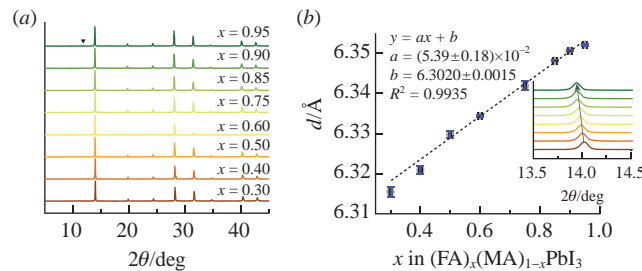


Figure 2 (a) X-ray diffraction patterns of $(\text{FA})_x(\text{MA})_{1-x}\text{PbI}_3$ powders with different x (black triangle indicates reflection of the $\delta\text{-FAPbI}_3$ phase). (b) Dependence of the lattice parameter d on the x value in $(\text{FA})_x(\text{MA})_{1-x}\text{PbI}_3$. The inset shows the shift of the (100) reflection of perovskite with increasing x .

⁸ Powder X-ray diffraction patterns were recorded on a Bruker Advance D8 diffractometer in the Bragg–Brentano geometry using $\text{CuK}\alpha$ radiation in the 2θ range of 5–45° with a step of 0.02°. The Rietveld refinement was performed using the JANA2006 software,²³ the standard uncertainty (indicated in Figure 2 as the y -axis error bar) was calculated to be 10^{-4} – 10^{-3} for all compositions.

results of approximation of the measured solubilities of organic halides in solutions in toluene with a higher concentration of I_2 , we assume that the concentration of organic cations is about 0.2 mM.

According to XRD data, all the obtained powders, except for one with $x = 0.95$, are single-phase [Figure 2(a)]. The most FA^+ -enriched composition contains a small admixture of the $\delta\text{-FAPbI}_3$ phase (the 2H polytype). Thus, $x = 0.95$ can be considered the boundary of the homogeneity region of $(\text{FA})_x(\text{MA})_{1-x}\text{PbI}_3$ solid solutions. On closer examination, one can notice a systematic shift of all reflections of the cubic perovskite phase towards smaller angles with increasing x . The Rietveld refinement revealed a linear increase in the unit cell parameter (d) with an increase in the FA^+ fraction [Figure 2(b)], which is explained by its larger size compared to MA^+ .

The resulting linear dependence $d(x)$ demonstrates excellent agreement with the similar one built for single crystals with allowance for the correction of the FA/MA ratio according to the NMR results.²⁰ In contrast to all other methods, in our method the cationic composition of the obtained powders exactly corresponds to the molar ratio of precursors: all initial reagents are completely converted into a homogeneous perovskite solid solution, and the liquid phase is capable of dissolving no more than 10^{-4} mmol of organic salts. The error in composition is determined only by the accuracy of weighing, therefore, in the case of sufficiently large samples, it can be completely eliminated.

The resulting powders were also characterized by photoluminescence (PL) spectroscopy at liquid nitrogen temperature.¹ This method makes it possible not only to determine the dependence of the emission maximum on the composition, but also to detect impurities of phases with different compositions, the PL of which is imperceptible at room temperature due to a small amount or is suppressed due to the transfer of excitation energy to a narrower-bandgap main phase.

As can be seen from Figure 3, the PL maximum gradually shifts towards lower energies from 1.604 eV for $x = 0.3$ to 1.484 eV for $x = 0.9$. At the same time, the PL band becomes more symmetric and loses its flatter slope toward the low-energy side of the maximum, which is characteristic of compositions enriched in MA^+ . It should be noted that the PL maximum shifts to the low-energy region almost linearly with an increase in the FA^+ fraction [Figure 3(b)]. The antibatic dependence of the PL maximum and the unit cell parameter on x indicates a linear decrease in the optical bandgap with increasing Pb–I bond length (half of the d parameter). The latter is explained by an increase in the efficiency of overlapping lead and iodine orbitals with a decrease in the tilting of PbI_6 octahedra with an increase in the unit cell parameter.^{21,22}

In summary, for the first time, we have developed a facile method for the synthesis of mixed-cation hybrid perovskite under thermodynamic equilibrium conditions without the use of solvents and high temperatures. The stoichiometry of the resulting

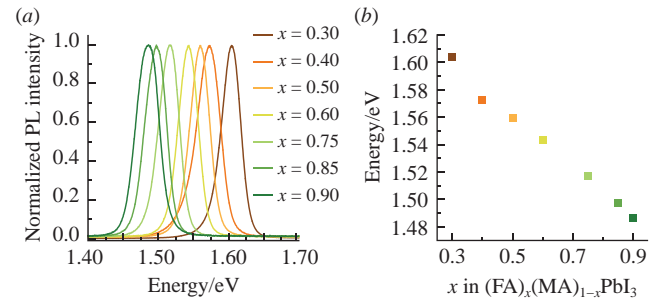


Figure 3 (a) Low-temperature PL spectra of the $(\text{FA})_x(\text{MA})_{1-x}\text{PbI}_3$ powders. (b) Dependence of the position of the PL maximum on the composition of the powder.

¹ PL spectra at 77 K were recorded using a 405 nm laser as an excitation source and an Ocean Optics USB4000+ CCD spectrometer.

(FA)_x(MA)_{1-x}PbI₃ powders strictly corresponds to the target molar ratio of the initial precursors. As a result, the boundary of the homogeneity region of (FA)_x(MA)_{1-x}PbI₃ solid solutions was refined, and linear dependences of the unit cell parameter and the position of the PL maximum on the ratio of organic cations were obtained. The method allows not only to determine the true phase equilibria, but also opens up the prospect for facile production of convenient single-source precursors for complex mixed-cation and mixed-anion perovskite compositions.

This work was supported by the state task of M. V. Lomonosov Moscow State University ‘Investigation and development of new materials for solar energetics’. XRD measurements were performed using the equipment of the Joint Research Center for Physical Methods of Research of N. S. Kurnakov Institute of General and Inorganic Chemistry of the Russian Academy of Sciences (JRC PMR IGIC RAS).

Online Supplementary Materials

Supplementary data associated with this article can be found in the online version at doi: 10.1016/j.mencom.2023.04.004.

References

- 1 S. De Wolf, J. Holovsky, S.-J. Moon, P. Löper, B. Niesen, M. Ledinsky, F.-J. Haug, J.-H. Yum and C. Ballif, *J. Phys. Chem. Lett.*, 2014, **5**, 1035.
- 2 Q. Dong, Y. Fang, Y. Shao, P. Mulligan, J. Qiu, L. Cao and J. Huang, *Science*, 2015, **347**, 967.
- 3 B. R. Sutherland and E. H. Sargent, *Nat. Photonics*, 2016, **10**, 295.
- 4 Y. Fu, H. Zhu, J. Chen, M. P. Hauzinger, X.-Y. Zhu and S. Jin, *Nat. Rev. Mater.*, 2019, **4**, 169.
- 5 N.-G. Park and K. Zhu, *Nat. Rev. Mater.*, 2020, **5**, 333.
- 6 NREL, *Best Research-Cell Efficiency Chart*, <https://www.nrel.gov/pv/assets/pdfs/best-research-cell-efficiencies.20221206.pdf>.
- 7 T. J. Jacobsson, A. Hultqvist, A. García-Fernández, A. Anand, A. Al-Ashouri, A. Hagfeldt, A. Crovetto, A. Abate, A. G. Ricciardulli, A. Vijayan, A. Kulkarni, A. Y. Anderson, B. P. Darwich, B. Yang, B. L. Coles, C. A. R. Perini, C. Rehermann, D. Ramirez, D. Fairen-Jimenez, D. Di Girolamo, D. Jia, E. Avila, E. J. Juarez-Perez, F. Baumann, F. Mathies, G. S. A. González, G. Boschloo, G. Nasti, G. Paramasivam, G. Martínez-Denegri, H. Näsström, H. Michaelis, H. Köbler, H. Wu, I. Benesperi, M. I. Dar, I. Bayrak Pehlivan, I. E. Gould, J. N. Vagott, J. Dagar, J. Kettle, J. Yang, J. Li, J. A. Smith, J. Pascual, J. J. Jerónimo-Rendón, J. F. Montoya, J. P. Correa-Baena, J. Qiu, J. Wang, K. Sveinbjörnsson, K. Hirselandt, K. Dey, K. Frohma, L. Mathies, L. A. Castriotta, M. H. Aldamasy, M. Vasquez-Montoya, M. A. Ruiz-Preciado, M. A. Flatken, M. V. Khenkin, M. Grischek, M. Kedia, M. Saliba, M. Anaya, M. Veldhoen, N. Arora, O. Shargaieva, O. Maus, O. S. Game, O. Yudilevich, P. Fassl, Q. Zhou, R. Betancur, R. Munir, R. Patidar, S. D. Stranks, S. Alam, S. Kar, T. Unold, T. Abzieher, T. Edvinsson, T. W. David, U. W. Paetzold, W. Zia, W. Fu, W. Zuo, V. R. F. Schröder, W. Tress, X. Zhang, Y.-H. Chiang, Z. Iqbal, Z. Xie and E. Unger, *Nat. Energy*, 2022, **7**, 107.
- 8 B. Murali, H. K. Kollu, J. Yin, R. Ketavath, O. M. Bakr and O. F. Mohammed, *ACS Mater. Lett.*, 2020, **2**, 184.
- 9 A. A. Petrov, E. I. Marchenko, S. A. Fateev, L. Yumao, E. A. Goodilin and A. B. Tarasov, *Mendeleev Commun.*, 2022, **32**, 311.
- 10 S. Ruan, R. Fan, N. Pai, J. Lu, N. A. S. Webster, Y. Ruan, Y.-B. Cheng and C. R. McNeill, *Chem. Commun.*, 2019, **55**, 11743.
- 11 W. T. M. Van Gompel, R. Herckens, G. Reekmans, B. Ruttens, J. D’Haen, P. Adriaensens, L. Lutsen and D. Vanderzande, *J. Phys. Chem. C*, 2018, **122**, 4117.
- 12 B. Conings, J. Drijkonigen, N. Gauquelin, A. Babayigit, J. D’Haen, L. D’Olieslaeger, A. Ethirajan, J. Verbeeck, J. Manca, E. Mosconi, F. De Angelis and H.-G. Boyen, *Adv. Energy Mater.*, 2015, **5**, 1500477.
- 13 A. S. Tutantsev, N. N. Udalova, S. A. Fateev, A. A. Petrov, W. Chengyuan, E. G. Maksimov, E. A. Goodilin and A. B. Tarasov, *J. Phys. Chem. C*, 2020, **124**, 11117.
- 14 O. S. Voronin, A. Y. Grishko, Y. M. Finkelberg, A. A. Petrov, E. A. Goodilin and A. B. Tarasov, *J. Phys. Chem. Lett.*, 2022, **13**, 2695.
- 15 A. A. Petrov, I. P. Sokolova, N. A. Belich, G. S. Peters, P. V. Dorovatovskii, Y. V. Zubavichus, V. N. Khrustalev, A. V. Petrov, M. Grätzel, E. A. Goodilin and A. B. Tarasov, *J. Phys. Chem. C*, 2017, **121**, 20739.
- 16 A. Y. Grishko, A. A. Eliseev, E. A. Goodilin and A. B. Tarasov, *Chem. Mater.*, 2020, **32**, 9140.
- 17 N. N. Udalova, A. S. Tutantsev, S. A. Fateev, E. A. Zharenova, N. A. Belich, E. M. Nemygina, A. V. Ryabova, E. A. Goodilin and A. B. Tarasov, *Russ. J. Inorg. Chem.*, 2021, **66**, 153 (*Zh. Neorg. Khim.*, 2021, **66**, 149).
- 18 A. A. Petrov, S. A. Fateev, Y. V. Zubavichus, P. V. Dorovatovskii, V. N. Khrustalev, I. A. Zvereva, A. V. Petrov, E. A. Goodilin and A. B. Tarasov, *J. Phys. Chem. Lett.*, 2019, **10**, 5776.
- 19 E. A. Goodilin, A. B. Tarasov, N. A. Belich and P. A. Ivlev, *RU Patent 2779015*, 2022.
- 20 A. Pisani, C. Ferrara, P. Quadrelli, G. Guizzetti, M. Patrini, C. Milanese, C. Tealdi and L. Malavasi, *J. Phys. Chem. C*, 2017, **121**, 8746.
- 21 C. Katan, N. Mercier and J. Even, *Chem. Rev.*, 2019, **119**, 3140.
- 22 E. I. Marchenko, S. A. Fateev, A. A. Ordinartsev, P. A. Ivlev, E. A. Goodilin and A. B. Tarasov, *Mendeleev Commun.*, 2022, **32**, 315.
- 23 V. Petříček, M. Dušek and L. Palatinus, *Z. Kristallogr. – Cryst. Mater.*, 2014, **229**, 345.

Received: 28th December 2022; Com. 22/7075